A First Step Towards the Implementation and Software-to-Software Validation of an Active Distribution Network Model

Aboutaleb Haddadi, Hossein Hooshyar, Jean Mahseredjian, Christian Dufour, and Luigi Vanfretti

***Abstract*—This paper presents the implementation of an Active Distribution Network model and its qualitative appraisal using different off-line and real-time simulation tools. The objective is to provide a first step towards software-to-software verification for the establishment of the model as a potential benchmark. The Active Distribution Network has multiple voltage levels and features various types of distributed energy resources including solar, wind, and storage. It further incorporates control and protection schemes for distributed energy resource units and loads and, hence, can represent the complex dynamics of an active distribution grid. As such, the test system can be used by other researchers to test numerical methods and conduct research on Smart Grid control, protection, and dynamic studies.**

***Keywords*: Power system benchmark, electromagnetic transients, power system simulation, active distribution network, smart grid control, protection, power system modeling.**

I. Introduction

TEST power systems for simulation studies of active distribution grids are rare. The existing distribution grid benchmarks in the literature often operate at a single voltage level and lack components such as Distributed Energy Resources (DER) and protection systems; hence, they cannot adequately represent the complex dynamics of an active distribution grid. Reference [1] has presented a medium voltage (MV) and a low voltage (LV) distribution network benchmark for DER integration; both benchmarks operate at a single voltage level and do not contain DER units. Reference [2] has provided five distribution test feeders; although a number of them feature two voltage levels, they lack DER units and, hence, do not represent an active grid. Details of these test feeders are available online at [3]. Reference [4] has presented a test distribution feeder which operates at a single voltage level and lacks DER units.

This paper presents an Active Distribution Network (ADN) model developed for control, protection, and dynamic studies of active distribution grids integrating DER. The paper presents its implementations in two different software environments and compares the simulation results.

The original ADN model has been developed in MATLAB/Simulink [5] and modified for use in the Opal-RT real-time simulator using the stub-line simulation technique; this technique decreases the accuracy of solution in networks such as the proposed ADN where feeders are short. To overcome this challenge, another version of the test ADN has been developed using the state-space nodal analysis method (SSN) [6], which is a delay-free parallelization approach that can be utilized in the Opal-RT simulator. Reference [7] has shown that relevant differences exist between the results of the stub-line and the SSN versions and concludes that the stub-line technique is inadequate for real-time simulation of ADNs. The accuracy of the SSN version has been compared to that of an off-line (non-real-time) version of the grid model using the standard Simulink solvers used by Simscape Power Systems models [8]. The two model implementations are available online in the Github platform [9].

To further verify the ADN model implementations, this paper presents a new implementation within the EMTP-RV environment and compares the results to the existing SSN version. The EMTP-RV model is used for off-line simulations, contains no artificial delay blocks, and uses an iterative solver for nonlinear functions; thus, it provides additional results for simulation accuracy analysis. Furthermore, with EMTP-RV it is possible to start the simulations from an unbalanced power flow solution. The solution to the initialization problem provides initial conditions for time-domain simulation which is an important step when performing simulations; thus, the solution of the initialization problem is also compared.

It is a challenging task to develop two perfectly matching versions of a large-scale test system, such as the proposed ADN, in two different software environments. References [10] and [11] have shown that such a challenge may exist even in a small system with fewer components and even when the two models share the same control equations. One of the objectives of this paper is to highlight these challenges in the context of the proposed ADN, identify the causes of inconsistent results, and provide recommendations to reduce such differences. As such, this paper aims to serve as a first step towards matching the EMTP-RV and SSN versions. Work is in progress to further improve the consistency of the results from different versions of the ADN model.

The model presented in this paper and its simulation with different tools provides software-to-software verification for the establishment of the model as a potential benchmark. The model can be used by other researchers for testing numerical methods and conducting research on Smart Grid control, protection, and dynamic studies.

A. Haddadi and J. Mahseredjian are with Montreal Polytechnique, Montréal, QC H3T1J4 Canada (e-mail: aboutaleb.haddadi@polymtl.ca and jean.mahseredjian@polymtl.ca).

H. Hooshyar and L. Vanfretti are with KTH Royal Institute of Technology, Stockholm, Sweden (e-mail: hosseinh@kth.se and luigiv@kth.se).

Christian Dufour is with Opal-RT Technologies, Montréal, QC Canada (e-mail: christian.dufour@opal-rt.com)

Paper submitted to the International Conference on Power Systems Transients (IPST2017) in Seoul, Republic of Korea June 26-29, 2017

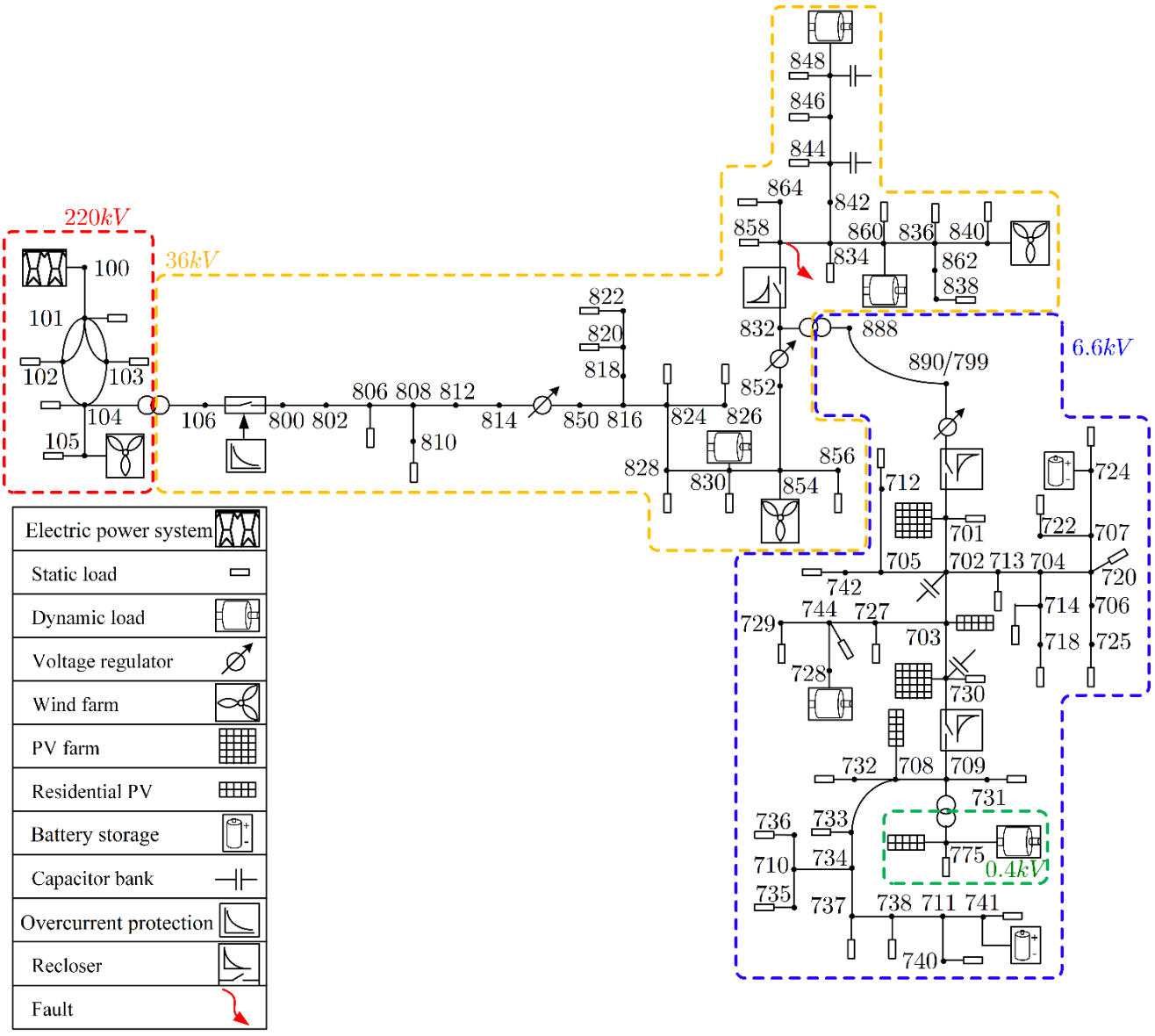

Fig. 1. Single-line diagram of the ADN.

II. The Active Distribution Network Model

Fig. 1 shows a single line diagram of the ADN which comprises 79 unbalanced buses. The model includes a 220-kV transmission grid (HV), a 36-kV medium-voltage (MV), a 6.6-kV low-voltage (LV), and a 0.4-kV residential LV grid. The total generation is 200MW, and the overall load of the modelled system is 191MW. The generation and load of the ADN (MV, LV, and residential LV grids) represent total DER generation of 5MW and load of 4.1MW+j1.9MVar; hence, the ADN can be operated as a micro grid. The DER includes wind, solar, and storage component models. The model of the DERs includes power electronic interfaces, control, and protection schemes. System loads include both three-phase and single-phase static loads as well as motor loads. The ADN model also includes voltage, current, and frequency protection schemes for DER units, feeders, and loads. Reference [5] presents the details of the component models.

It should be mentioned that the ADN model presented in this paper uses accurate time-domain models for all components and, therefore, may be used for the simulation of fast electromagnetic transient events under adequate assumptions[1].

Due to the complexity of the model, the size of the system of equations is large, and thus, the real-time simulation of the ADN is computationally demanding. References [5] and [7] have developed two versions of the test ADN for real-time simulations in the Opal-RT simulator which employ the stub-line and SSN techniques, respectively. The next sections briefly present these two implementations for the sake of completeness.

A. Stub-line Implementation

Reference [5] has presented the stub-line version in which the model is split into 11 subsystems by inserting 7 stub-line blocks at distribution feeder sections 816-824, 854-852, 858-834, 701-702, 713-704, 703-730, and 733-734, two stub-line

[1] Note that certain components and portions of the model are represented with lumped parameter models, and thus, some electromagnetic transient phenomena cannot be represented without modifying the model accordingly.

transformer blocks at 104-106 and 832-888, and one ARTEMiS distributed parameters line block (based on Bergeron's travelling wave line model) at the transmission line section 100-101. The stub-lines represent part of the distribution feeder by an N-phase transmission line model with exactly one time-step propagation delay [12]; this artificial propagation delay decouples the state-space equation system of the network on the two sides which allows the real-time simulation of ADN to be performed on 11 cores in parallel. Nevertheless, the stub-line blocks negatively impact the simulation accuracy of the ADN due to the approximation involved in representing a short feeder partially by a transmission line model. Reference [7] has shown these accuracy issues and developed another implementation using the delay-free SSN technique.

B. SSN Implementation

The SSN version partitions the grid model into 11 SSN groups (HV section into 2 groups, MV section into 4 groups, and LV and residential LV sections into 5 groups). The SSN solver then uses a threaded process to compute the groups in parallel without the need for any artificial delay between them. The SSN version keeps the two stub-line transformer blocks at sections 104-106 and 832-888 since the existing leakage inductance of typical power system transformers is large enough to produce a small equivalent capacitance in the stub-line; Hence, they do not reduce the accuracy of solution.

Reference [7] has shown that the SSN version provides a more accurate solution compared to the stub-line version by comparing the results to an off-line delay-free model of the ADN in MATLAB/Simulink. To provide further results for simulation accuracy analysis, the next section presents another implementation in EMTP-RV.

III. EMTP-RV Implementation

The EMTP-RV version is for off-line simulations, contains no artificial delay blocks, and uses an iterative solver for nonlinear functions; thus, it provides additional results for simulation accuracy analysis.

A number of differences exist between the EMTP-RV, the stub-line, and SSN models. The first is the method of initialization of the time-domain solver. In the stub-line and SSN versions, two auxiliary ideal voltage sources are placed at the nodes 104 and 890/799 at simulation startup (i.e., the first 10 seconds of simulation) to help the grid model reach a stable operating point. In EMTP-RV, it is possible to initialize the time-domain simulation from an unbalanced power flow solution, and therefore there is no need for the artificial ideal voltage sources. Further, the loads in the SSN implementation include time-varying small random variations and other variations (sinusoidal) which have not been incorporated in the EMTP-RV version. These variations are needed for real-time hardware-in-the-loop studies used to test PMU applications where random loads excite important system dynamics [13]. In the SSN version, the loads have been modeled as constant-power, constant current, or constant impedance loads whereas in the EMTP-RV version, loads have been modeled by their constant-impedance RLC representation for simplicity. The same load models as in the SSN version are available in EMTP-RV and can be incorporated in the future EMTP-RV versions of the ADN. Further than the above-mentioned differences, the control and power schemes of PV and wind generation units are different in the SSN and EMTP-RV versions although their parameters have been adjusted to ensure similar real and reactive power outputs in a steady-state.

Table 1 presents a summary of the network data of the EMTP-RV model of the ADN.

TABLE 1: NETWORK DATA SUMMARY OF THE EMTP-RV MODEL OF THE ADN

Total number of network nodes	978
Size of the main system of equations	1617
Number of iterations per time-point	3.06

To analyze the differences between different implementations, the results of the EMTP-RV version have been compared to those of the SSN version. Since the accuracy issues of the stub-line implementation have been demonstrated in [7], this paper does not present the results of the stub-line version. Three sets of simulation results have been provided: power-flow solution; steady-state solution; and time-domain solution.

A. Power-flow Solution

The power-flow solution obtained in EMTP-RV is presented in Appendix. As shown, the voltage amplitude is between 0.95 to 1.02 pu indicating that the power-flow solution is acceptable. The power-flow solution illustrates that the ADN is unbalanced due to the presence of unbalanced three-phase loads, single-phase loads, and single-phase residential PV units.

It should be mentioned that the power-flow solution of EMTP-RV cannot be compared to that of the stub-line or SSN versions due to the presence of artificial ideal voltage sources in the stub-line and SSN versions used for initialization. These voltage sources act as slack buses imposing a different set of power-flow constraints than that of the EMTP-RV model.

B. Steady-State Solution

To compare the steady-state solution, the EMTP-RV model and the SSN model were run in time-domain for a sufficiently long time until an equilibrium operating point was reached. Table 2 compares the steady-state solutions for a number of selected buses.

TABLE 2: COMPARISON OF THE STEADY-STATE SOLUTION OF EMTP-RV VS. SSN: VOLTAGES ARE IN P.U.; PHASE ANGLES ARE IN DEGREES

Bus	quantity	EMTP-RV	SSN
852	V_a	1.03	1.03
	θ_a	21.0	22.0
	V_b	1.03	1.03
	θ_b	-99.0	-98.0
	V_c	1.03	1.03
	θ_c	141.0	142.0
799	V_a	1.02	1.02
	θ_a	18.0	20.0
	V_b	1.02	1.02
	θ_b	-102.0	-100.0
	V_c	1.02	1.02
	θ_c	138.0	140.0
730	V_a	1.01	1.01
	θ_a	18.0	20.0
	V_b	1.01	1.02
	θ_b	-102.0	-100.0
	V_c	1.01	1.01
	θ_c	138.0	140.0

As shown, the voltages match closely while the phase angles exhibit a slight difference. This difference is primarily due to different load models used in the two versions; in the SSN version, static loads have been modeled by their constant-power, constant-impedance, or constant-current representation whereas in the EMTP-RV model, they have been modeled by an equivalent RLC representation. Consequently, they draw slightly different real and reactive power in the two versions. As a future work, this difference can be further reduced by using the same load models in the EMTP-RV version. The load models are available in EMTP-RV.

C. Time-domain Simulation

To compare time-domain results, a 6-cycle three-phase bolted fault is applied on the MV feeder at bus 858 at t = 50 s. Subsequently, the three-phase MV recloser at the feeder section 832-858 detects and isolates the fault within 2 cycles.

Fig. 2(a) shows the voltage (phase 'a') of bus 832 of the MV section obtained using the SSN and EMTP-RV models, and Fig. 2(b) illustrates the first 5 seconds following the fault.

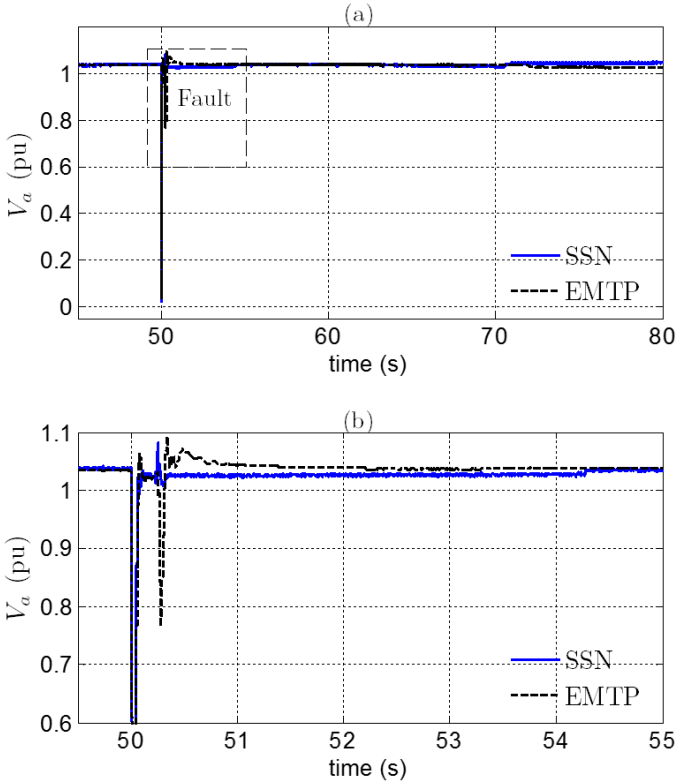

Fig. 2. Voltage (phase 'a') of bus 832 of the MV section in response to a three-phase bolted fault on bus 858 at t = 50 s obtained from the stub-line, the SSN, and the EMTP-RV model.

Fig. 3(a) depicts a closer view of the voltage in the first few cycles following the fault, and Fig. 3(b) shows the breaker signal of the MV recloser at the feeder section 832-858. As shown, the overcurrent protection detects the fault and issues the trip signal at 50.033 s in both the EMTP-RV and the SSN models. The reclosing takes place at 50.2332 s in EMTP-RV compared to 50.2331 s in the SSN model. As Fig. 2 and Fig. 3 show, the time-domain results of the EMTP-RV version and the SSN version exhibit similarities and differences; the tripping and reclosing times shown in Fig. 3(b) match closely whereas the voltage overshoot and undershoot are slightly different. These differences are primarily due to the difference in the parameters of the control and power schemes of the DER units of the EMTP-RV and SSN versions which result in a different transient behavior. As mentioned earlier, the EMTP-RV model of the DER units only matches the steady-state real- and reactive-power output of those of the SSN version which does not guarantee a similar dynamic characteristic. As a future work, the control of DER units is to be adjusted to make the time-domain results of the two versions more consistent. It is expected that DER units with larger ratings should have a more significant impact on the transient response of the system, and thus, their control parameters should be adjusted first.

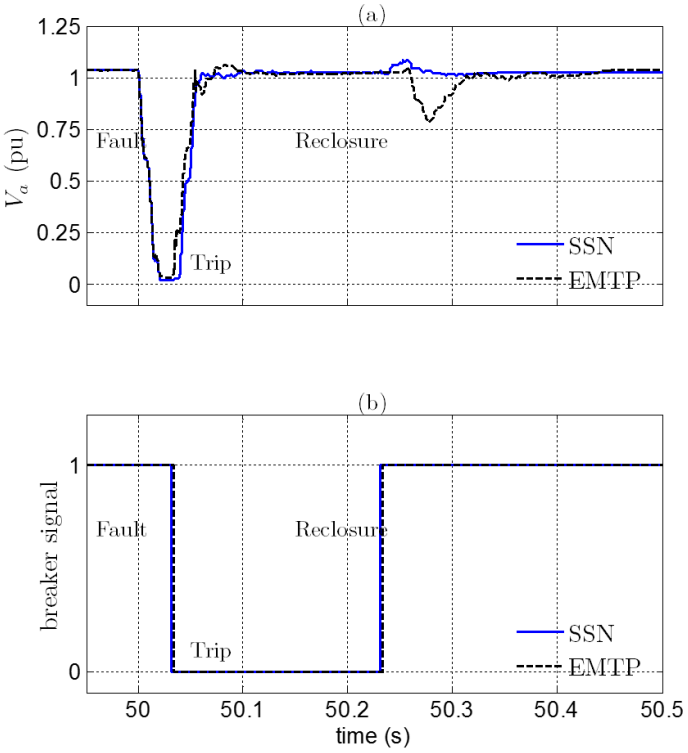

Fig. 3. A three-phase bolted fault on bus 858 at t = 50 s obtained from the stub-line, the SSN, and the EMTP-RV model: (a) voltage (phase 'a') of bus 832 and (b) the breaker signal of the MV recloser at the feeder section 832-858.

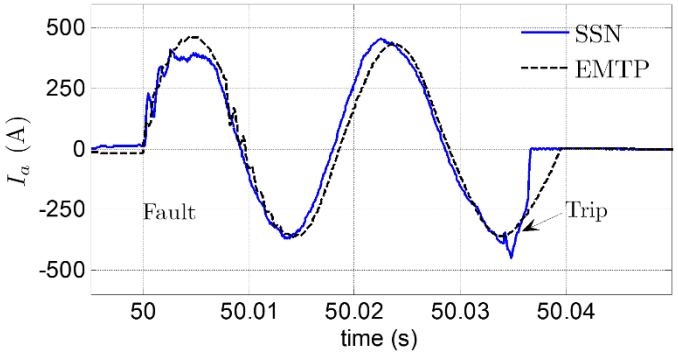

Fig. 4. Fault current (phase 'a') for a three-phase bolted fault at t=50 s on bus 858 obtained from the SSN and the EMTP-RV model.

Fig. 4 shows the fault current (phase 'a') obtained from the SSN and the EMTP-RV models. The fault current waveforms have been obtained assuming no load variations in the SSN and EMTP-RV versions. As shown, the fault current exhibits some differences in the first cycle in terms of peak instantaneous current and the amplitude and frequency of high-frequency oscillations; the fault currents become more comparable in the second cycle. These differences

predominately stem from the difference in control parameters of DER units as their time-scale of milliseconds corresponds to the time-constant of the control scheme of the DER units. Furthermore, the current waveforms exhibit a phase difference which is most likely due to the difference in the time-constant of the real- and reactive-power control scheme of the DER units.

It should be mentioned that conducted simulation tests showed that the results of the stub-line version becomes more comparable to the SSN and EMTP-RV versions when one reduces the under-voltage protection setting of loads and the stall voltage limit of motor loads in the stub-line version.

D. Discussion

As mentioned in the previous section, the EMTP-RV and SSN versions do not provide perfectly matching results. The differences are most likely due to modeling differences since in theory, SSN and EMTP-RV are expected to give the same solution if the two models match perfectly [6]. Nevertheless, it is a challenging task to match the two models given the complexity of the model and the large number of components used in the model. The main objective of this paper is to highlight the difficulty of matching different versions of a system modeled in different simulation environments. Reference [10] has provided a systematic method to assess discrepancies between simulation tools, and [11] has developed a method to achieve a higher consistency between different time-domain simulation tools. These two references have shown that achieving perfectly matching results is a challenge even when the two models share the same control equations in a source code. This paper does not claim to have achieved a perfect match between the EMTP-RV and the SSN versions; rather it is expected to serve as a first step towards achieving such objective.

As a future work to achieve a higher consistency between the two models, one solution is to employ a bottom-up systematic methodology by decomposing the full model into small parts, cross-examining the small parts individually, and then cross-examining the model as a whole. This decomposition can be done at functional parts level, i.e., the HV, MV, and LV subsystems, and at principle parts level, i.e., control and power circuits. The power circuit of individual parts can be tested by disabling the control circuit (e.g., by imposing such conditions as fixed rotor speed for motors, and setting off the on-load-tap-changer regulator). Then the control circuit can be activated to check differences in control.

IV. Conclusions

This paper has presented an Active Distribution Network test system for Smart Grid control, protection, and dynamic studies. Three implementations of the test system were presented: an EMTP-RV implementation for off-line simulations; a delay-based stub-line version and a delay-free SSN version for real-time simulations. The paper has compared the EMTP-RV and the SSN models in terms of their steady-state and time-domain dynamic behavior. The results of the stub-line version have not been presented since they have been shown to be inaccurate [6]. The paper has qualitatively shown that the EMTP-RV and the SSN versions give simulation results with acceptable agreement, and hence, serves as a first step towards software-to-software validation of the test ADN. The results of the two versions also exhibit some differences due to modeling differences. The paper has explained these differences, identified their cause, and provided recommendations to reduce them. To improve the consistency of the results, it is recommended to take a systematic bottom-up approach whereby the individual components are cross-checked first and then the overall model is matched in the two software environments. Future work includes investigating this approach to further improve the consistency of results.

Conducted simulation tests showed that it is necessary to adjust the parameters of the stub-line version to make results more comparable to the EMTP-RV and SSN versions.

V. Appendix

Table 3 presents the power-flow solution of the ADN obtained in EMTP-RV.

VI. References

[1] CIGRE Task Force C6.04.02, CIGRE Tech. Brochure, "Benchmark systems for network integration of renewable and distributed energy resources," 2011.

[2] W.H. Kersting, "Radial distribution test feeders," in *IEEE PES Winter Meeting*, 2001.

[3] http://www.ewh.ieee.org/soc/pes/dsacom/testfeeders/index.html

[4] J.S. Savier, D. Das, "Impact of network reconfiguration on loss allocation of radial distribution system," *IEEE Trans. Power Del.*, vol. 22, no. 4, pp. 2473–2480, Oct. 2007.

[5] H. Hooshyar, F. Mahmood, L. Vanfretti, and M. Baudette, "Specification, implementation, and hardware-in-the-loop real-time simulation of an active distribution grid," *Sustainable Energy, Grids and Networks*, vol. 3, pp.36–51 Sep. 2015.

[6] C. Dufour, J. Mahseredjian and J. Bélanger: "A combined state-space nodal method for the simulation of power system transients," *IEEE Trans. Power Del.*, vol. 26, no. 2, pp. 928–935, Apr. 2011.

[7] H. Hooshyar, L. Vanfretti, C. Dufour, "Delay-free parallelization for real-time simulation of a large active distribution grid model," in *Proc. IEEE IECON*, Italy, Oct. 2016.

[8] https://www.mathworks.com/help/physmod/sps/

[9] Hossein Hooshyar and Luigi Vanfretti (2016). FP7-IDE4L-KTHSmarTSLab-ADN-RTModel: First Release [Data set]. Sustainable Energy, Grids and Networks. Zenodo. http://doi.org/10.5281/zenodo.61183

[10] R. Rogersten, L. Vanfretti, W. Li, L. Zhang, and P. Mitra, "A quantitative method for the assessment of VSC-HVdc controller simulations in EMT tools," in *Innovative Smart Grid Technologies Cotiference Europe* (*ISGT-Europe*), 2014 1EEE PES, vol. 1, no. 5, pp. 12-15, Oct. 2014.

[11] R. Rogersten, L. Vanfretti, and W. Li, "Towards consistent model exchange and simulation of VSC-HVdc controls for EMT studies," in *IEEE ISGT 2015*, Washington DC, USA, 2015.

[12] H. Dommel, "Digital computer solution of electromagnetic transients in single and multiple networks," *IEEE Trans. Power Apparatus and Syst.*, vol. PAS-88, no. 4, pp. 388–399, Apr. 1969.

[13] R. S. Singh, M. Baudette, H. Hooshyar, L. Vanfretti, M. S. Almas, S. Løvlund, "'In Silico' testing of a decentralized PMU data-based power systems mode estimator," in *Proc. IEEE PES General Meeting*, Boston, MA, US, July 17-21, 2016.

TABLE 3
POWER-FLOW SOLUTION OF THE ADN IN EMTP-RV

Bus	Phase a		Phase b		Phase c		Bus	Phase a		Phase b		Phase c	
	V (pu)	Phase angle (deg)	V (pu)	Phase angle (deg)	V (pu)	Phase angle (deg)		V (pu)	Phase angle (deg)	V (pu)	Phase angle (deg)	V (pu)	Phase angle (deg)
100	1.02	-1.9	1.02	-121.9	1.02	118.1	741	0.97	16.2	0.97	-103.7	0.97	136.2
101	0.99	-10.5	0.99	130.5	0.99	109.5	742	0.98	16.1	0.98	-103.8	0.97	136.3
102	0.99	-11.8	0.99	-131.8	0.99	108.2	744	0.98	16.2	0.98	-103.8	0.98	136.3
103	0.99	-12.1	0.99	-132.1	0.99	108.0	775	0.98	16.3	0.98	-103.8	0.98	136.2
104	0.99	-12	0.99	-132.0	0.99	108.0	800	0.98	16.8	0.98	-103.1	0.99	137.1
105	1.00	-10.5	1.00	-130.5	1.00	109.5	802	0.98	16.8	0.98	-103.1	0.99	137.1
106	0.98	16.8	0.98	-103.1	0.99	137.1	806	0.98	16.8	0.98	-103.1	0.99	137.1
701	0.98	16.2	0.98	-103.8	0.98	136.2	808	0.97	16.6	0.98	-103.3	0.99	136.9
702	0.98	16.2	0.98	-103.8	0.98	136.2	810	n.a.	n.a.	0.98	-103.3	n.a.	n.a.
703	0.98	16.2	0.98	-103.8	0.98	136.3	812	0.96	16.4	0.97	-103.6	0.98	136.8
704	0.98	16.1	0.98	-103.8	0.97	136.2	814	0.95	16.2	0.97	-103.8	0.98	136.6
705	0.98	16.1	0.98	-103.8	0.97	136.2	816	0.99	16.2	1.00	-103.8	1.01	136.6
706	0.98	16.2	0.98	-103.8	0.97	136.2	818	0.99	16.2	n.a.	n.a.	n.a.	n.a.
707	0.98	16.2	0.97	-103.8	0.97	136.3	820	0.99	16.2	n.a.	n.a.	n.a.	n.a.
708	0.98	16.3	0.98	-103.8	0.97	136.2	822	0.99	16.2	n.a.	n.a.	n.a.	n.a.
709	0.98	16.3	0.98	-103.8	0.98	136.2	824	0.99	16.2	1.00	-103.8	1.00	136.5
710	0.97	16.2	0.97	-103.7	0.97	136.3	826	n.a.	n.a.	1.00	-103.8	n.a.	n.a.
711	0.97	16.2	0.97	-103.8	0.97	136.2	828	0.99	16.2	1.00	-103.8	1.00	136.5
712	0.98	16.1	0.98	-103.8	0.97	136.2	830	0.98	16.1	0.99	-103.9	1.00	136.4
713	0.98	16.1	0.98	-103.8	0.97	136.2	832	1.00	16.1	1.01	-104.0	1.01	136.1
714	0.98	16.1	0.98	-103.8	0.97	136.2	834	1.00	16.0	1.01	-104.1	1.01	135.9
718	0.98	16.1	0.98	-103.8	0.97	136.2	836	1.00	16.0	1.01	-104.1	1.01	135.9
720	0.98	16.1	0.98	-103.8	0.97	136.2	838	n.a.	n.a.	1.01	-104.1	n.a.	n.a.
722	0.97	16.2	0.97	-103.9	0.97	136.4	840	1.00	16.0	1.01	-104.1	1.01	135.9
724	0.97	16.3	0.97	-103.8	0.97	136.2	842	1.00	16.0	1.01	-104.1	1.01	135.9
725	0.98	16.2	0.98	-103.8	0.97	136.2	844	1.00	16.0	1.01	-104.1	1.01	135.9
727	0.98	16.2	0.98	-103.8	0.98	136.3	846	1.00	16.0	1.01	-104.2	1.01	135.9
728	0.98	16.2	0.98	-103.8	0.98	136.3	848	1.00	16.0	1.01	-104.2	1.01	135.9
729	0.98	16.2	0.98	-103.8	0.98	136.3	850	0.99	16.2	1.00	-103.8	1.01	136.6
730	0.98	16.2	0.98	-103.8	0.98	136.3	852	0.97	16.1	0.98	-104.0	0.98	136.1
732	0.98	16.3	0.98	-103.8	0.97	136.2	854	0.98	16.1	0.99	-103.9	1.00	136.4
733	0.97	16.3	0.97	-103.8	0.97	136.2	856	n.a.	n.a.	0.99	-103.9	n.a.	n.a.
734	0.97	16.2	0.97	-103.8	0.97	136.3	858	1.00	16.1	1.01	-104.1	1.01	136.0
735	0.97	16.2	0.97	-103.7	0.97	136.3	860	1.00	16	1.01	-104.1	1.01	135.9
736	0.97	16.3	0.97	-103.7	0.97	136.2	862	1.00	16	1.01	-104.1	1.01	135.9
737	0.97	16.2	0.97	-103.7	0.97	136.3	864	1	16.1	n.a.	n.a.	n.a.	n.a.
738	0.97	16.2	0.97	-103.8	0.97	136.3	888	1.00	16	1.01	-104.1	1.01	135.9
740	0.97	16.2	0.97	-103.7	0.97	136.2	890/799	0.95	16.2	0.95	-103.8	0.95	136.2